Deformation mapping in Lorentz transmission electron microscopy images of magnetic skyrmion lattices

Thibaud Denneulin, András Kovács and Rafal E. Dunin-Borkowski

Ernst Ruska Centre for Microscopy and Spectroscopy with Electrons, Forschungszentrum Jülich, 52425 Jülich, Germany.

JÜLICH Forschungszentrum

t.denneulin@fz-juelich.de

Introduction

Magnetic skyrmions are quasi-particles with a swirling spin texture. They have raised interest because of their potential applications in the field of spintronics, for instance in neuromorphic computing where they are treated as neurotransmitters in artificial synapses [1]. In chiral magnets, skyrmions are stabilized by the balance between the exchange interaction and the Dzaloshinskii-Moriya interaction and they can form 2D hexagonal lattices [2]. Similarly to atomic lattices, skyrmion lattices can exhibit local deformations and crystalline defects such as dislocations and grain boundaries depending on the geometric constraints and the external magnetic fields [3]. Measuring deformations in skyrmion lattices is important to understand the interplay between the lattice structure, the sample geometry and external influences.

In a hexagonal lattice, each skyrmion has normally 6 neighbors. However, it is common to observe dislocations formed by a pair of 5 and 7-coordinated skyrmions. Figure 1 shows an example of a Lorentz TEM image of a skyrmion lattice recorded in a 150 nm thick lamella of FeGe at 230 K with a defocus of 800 µm and in the presence of an external magnetic field of 145 mT. A dislocation is present in the middle of the image where a heptagon and a pentagon have been drawn. The dislocation introduces two half planes indicated by dashed lines. A Burgers circuit has also been traced to show the Burgers vector ***b***.

Figure 1

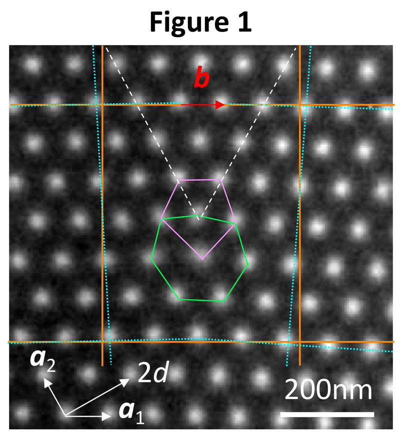

[1] K. M. Song *et al.*, *Nature Electronics* 3, 148-155 (2020)
[2] S. Mühlbauer *et al.*, *Science* 323, 915–919 (2009)
[3] T. Denneulin *et al.*, *Scientific Reports* 14, 12286 (2024)

Displacement and deformation fields around a dislocation

GPA is a lattice deformation analysis technique based on Fourier transform operations and primarily used in atomic resolution TEM images. A Fourier transform of the image is first calculated and numerical apertures are applied to a pair of Bragg spots with non-colinear reciprocal lattice **g**-vectors. After inverse Fourier transform, the geometric phase term $\phi(\mathbf{r})=-2\pi\mathbf{g}.\mathbf{u}(\mathbf{r})$ associated to each **g**-vector is retrieved, where **u** is the displacement vector.

Figure 2(a) shows a Fresnel image of a skyrmion lattice in FeGe that contains a dislocation. The Fourier transform is shown in Fig. 2(b). Cosine apertures were applied to two Bragg spots with reciprocal lattice vectors g_1 and g_2 as shown schematically by red circles. Figure 2(c,d) shows the sets of lattice fringes obtained after inverse FFT and Fig. 2(e,f) shows the corresponding geometric phase images ϕ_{g1} and ϕ_{g2}. The displacement along the horizontal and vertical directions can then be calculated by combination of the phase images.

Figure 2

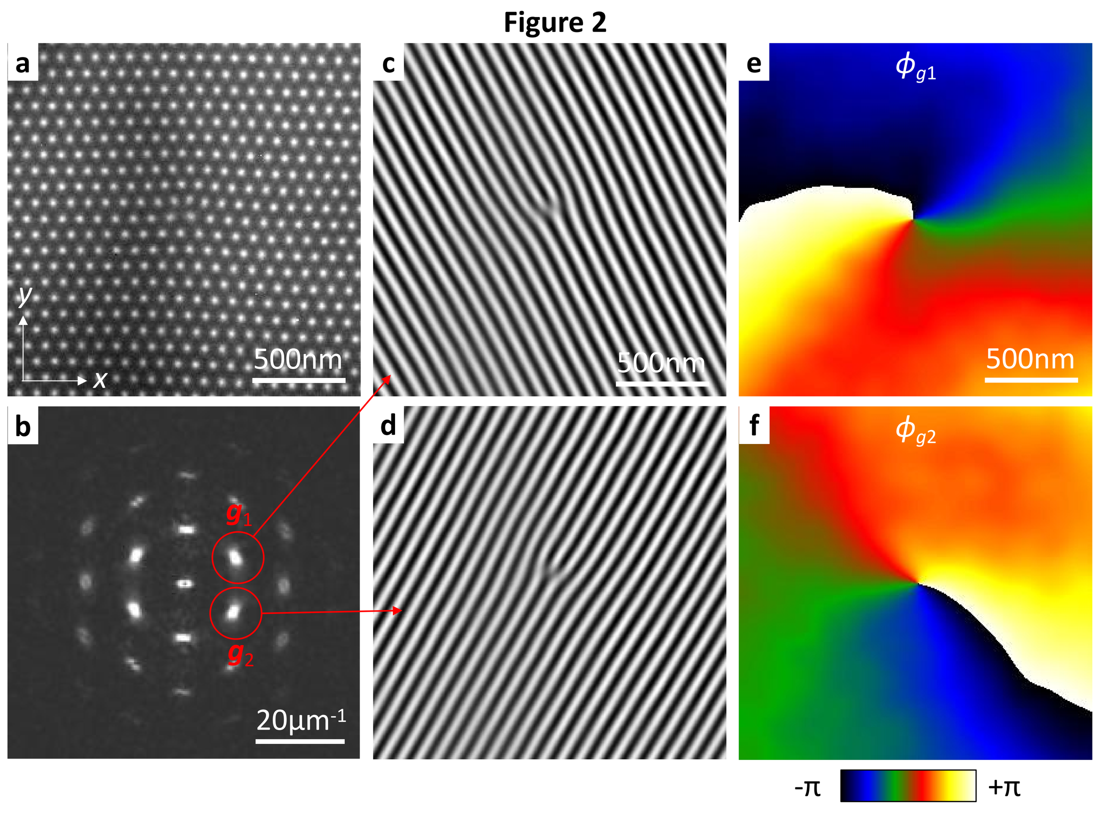

Figure 3(a,b) shows the horizontal u_x and vertical u_y components of the displacement fields. The u_x component varies circularly around the dislocation core. The u_y component is positive near the middle of the image and negative on the left and right sides. This can be understood by looking at the solid and dotted lines in Fig. 1. The vertical and horizontal planes are slightly tilted anti-clockwise on the left side of the image and clockwise on the right side. For comparison, theoretical displacement fields in Figure 3(c,d) were calculated using linear elastic theory following the expression

$$u_x = \frac{b}{2\pi}\left(\arctan(y,x) + \frac{xy}{2(1-\nu)(x^2+y^2)}\right)$$

$$u_y = \frac{b}{8\pi(1-\nu)}\left((1-2\nu)\ln(x^2+y^2) + \frac{x^2-y^2}{x^2+y^2}\right)$$

and using a Poisson ratio of $\nu = 1/3$ [2].

Figure 3

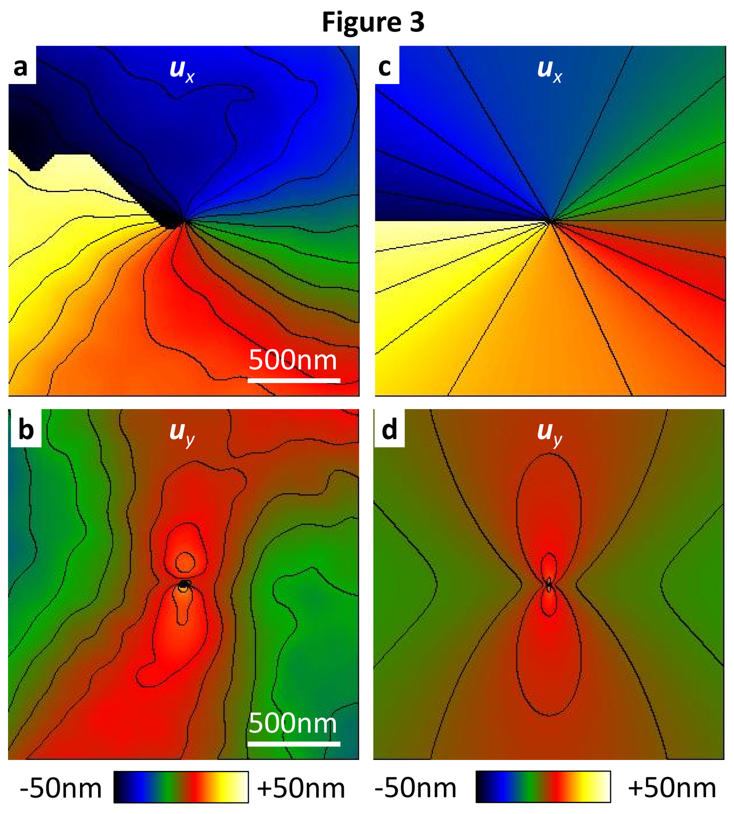

The deformation are then obtained using differentiation of the displacement field. Figure 4(a-d) shows the experimental deformation fields calculated using GPA and Figure 4(e-h) shows the corresponding theoretical deformation fields calculated from linear elastic theory. The horizontal deformation ε_{xx} along the direction parallel to the Burgers vector, shows a butterfly shape with negative (compressive) deformation in the top part of the image and positive (tensile) deformation in the bottom part. The vertical deformation ε_{yy} shows a three-fold symmetry with alternating negative and positive deformations around the dislocation core. The shear deformation ε_{xy} and the rigid-body rotation ω_{xy} show primarily loops oriented along the horizontal direction, parallel to the Burgers vector. Visually, the shape of the experimental and theoretical deformation fields is in good agreement even though the experimental images show some random fluctuations. For quantitative comparison, Fig. 4(i-l) shows the difference between the experimental and theoretical deformation fields.

$$\varepsilon_{xx} = \frac{\partial u_x}{\partial x}$$

$$\varepsilon_{yy} = \frac{\partial u_y}{\partial y}$$

$$\varepsilon_{xy} = \frac{1}{2}\left(\frac{\partial u_x}{\partial y} + \frac{\partial u_y}{\partial x}\right)$$

$$\omega_{xy} = \frac{1}{2}\left(\frac{\partial u_y}{\partial x} - \frac{\partial u_x}{\partial y}\right)$$

Figure 4

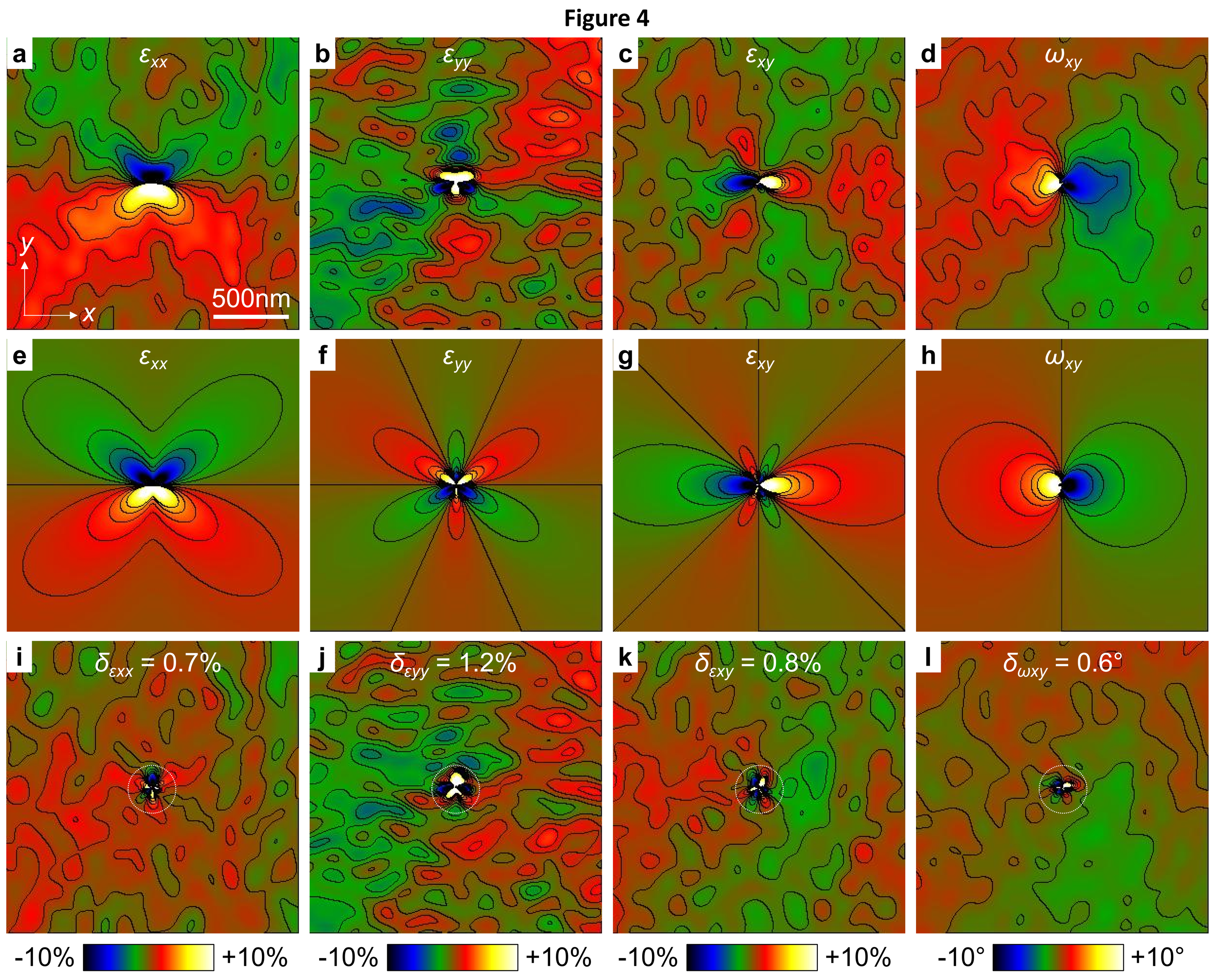

Rotation fields at grain boundaries

Grain boundaries consist of arrays of dislocations and the rotation between the grain depends on the density of dislocations. Figure 5(a) is a Fresnel image of a skyrmion lattice obtained at 235 K in the presence of an external field of 233 mT. It shows three skyrmion crystal grains labeled G1, G2 and G3 separated by 5-7 dislocation arrays, which are numbered on the image. The grain boundaries GB12 and GB23 show a relatively low density with clearly separated dislocations, whereas GB13 shows a high density with strictly alternating pentagons and heptagons. Figure 5(b) is the rigid-body rotation map ω_{xy} obtained using GPA and using the grain G1 as the reference. Figure 5(c) shows three rotation profiles extracted from the maps perpendicular to the grain boundaries and averaged along the grain boundaries as shown by dotted rectangles in the map. Rotations of ω_{xy} = 10°, 15° and 30° were measured for GB12, GB23 and GB13 respectively, with a precision of ± 1°. For comparison, a model was calculated in Fig. 5(d) by summing the rotation fields of individual dislocations. In isotropic elastic theory, the rotation field of an edge dislocation can be described in polar coordinates $\omega = -b\cos(\varphi)/2\pi r$. To create the model, the position and the orientation of the dislocations were measured from the experimental images. Profiles extracted from the model across the grain boundaries (dashed lines) have been reported in Fig. 5(c).

Figure 5

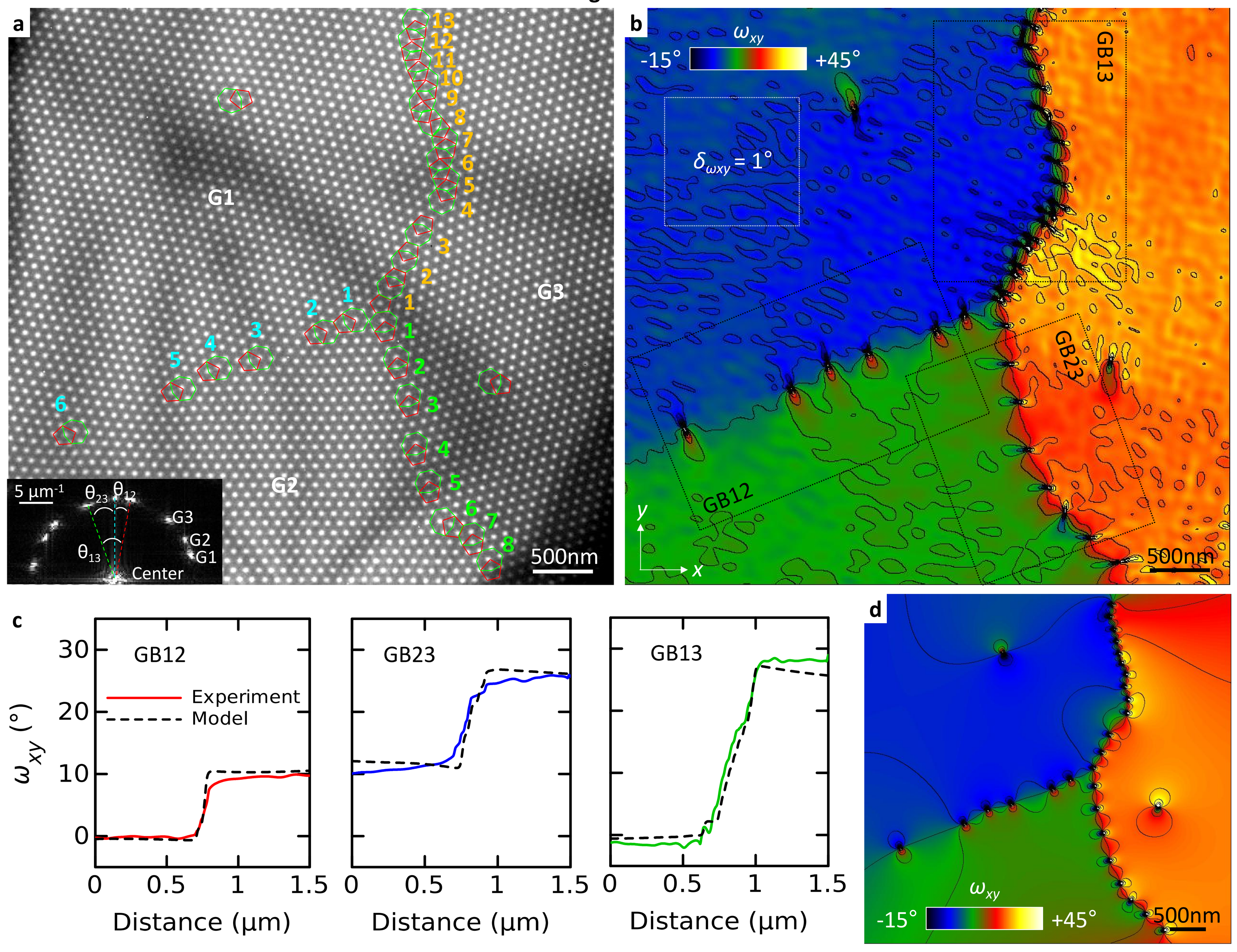

Evolution of deformation fields in magnetic field series

The density of defects and hence the disorder increase with the external magnetic field. Figure 6(a-d) shows Fresnel images of a skyrmion lattice obtained at 145mT, 291mT, 326mT and 340mT. In order to map the evolution of the disorder, we have calculated two types of maps. Figure 6(e-h) shows orientational maps obtained using the rigid-body rotation ω_{xy} and Fig. 6(j-m) shows maps of the hexagonality obtained by summing the different deformation components. The hexagonality is defined $1-|\varepsilon|$ with $|\varepsilon| = |\varepsilon_{xx}-\varepsilon_{yy}|/2 + |\varepsilon_{xy}+\varepsilon_{yx}|/2$. It is equal to 1 when there is no deformation and less than 1 in the presence of deformations. The standard deviation of the rotation $\delta\omega_{xy}$ and the mean value of the hexagonality parameter $\langle 1-|\varepsilon|\rangle$ are indicated on the maps. At low fields (145mT and 291mT), the maps are relatively uniform, $\delta\omega_{xy}$ is small and $\langle 1-|\varepsilon|\rangle$ is close to 1. At 326mT, the rotation map shows two large domains on the left and right sides of the image with a relative tilt of approximately 10°. At 340mT, multiple small domains with different orientations are visible with a large density of dislocations. Consequently, $\delta\omega_{xy}$ increases (6.2° at 326mT and 13.2° at 340mT) and $\langle 1-|\varepsilon|\rangle$ decreases significantly (respectively 0.93 and 0.80).

Figure 6

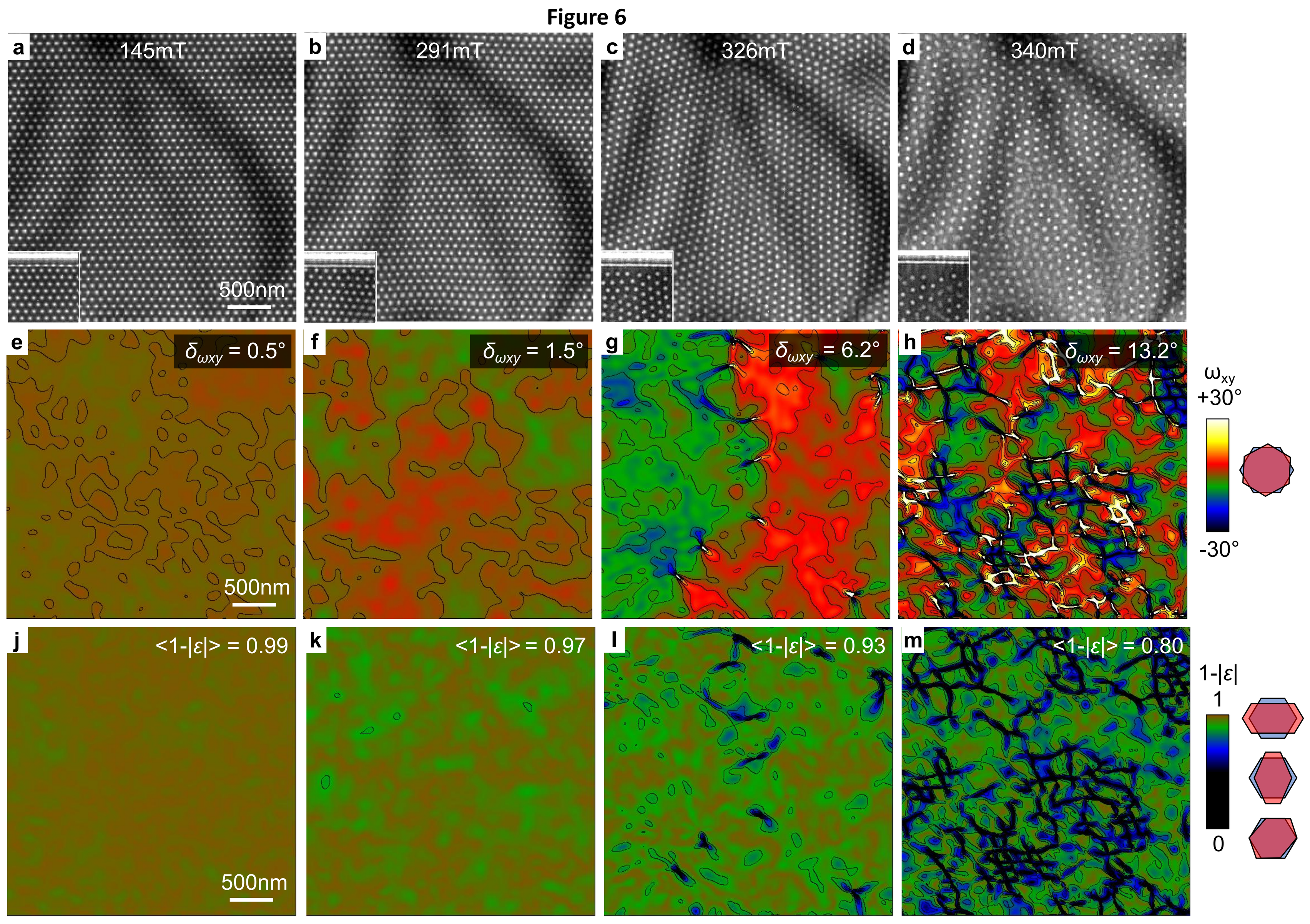

An orientational order ψ parameter and the corresponding correlation function G can also be derived from these maps. At 145mT and 291mT, the G plots show constant profiles close to 1 indicating a long-range orientational order, which is characteristic of a *solid* phase. At 326 mT, the profile decays continuously from 0.9 to 0.6 at 3 µm distance. It suggests that a degree of organization persists over intermediate distances, which points towards a quasi-long range order and an intermediate phase. At 340 mT, the profile decays rapidly to low values of 0.2-0.3 at 0.5 µm distance. It indicates a short-range order characteristic of a *liquid* phase.

$$\Psi(r) = (1-|\varepsilon|(r))\exp(i6\omega_{xy}(r))$$

$$G(r) = \frac{1}{N_r^{\mathrm{pix}}}\sum_{i,j}^{N_r^{\mathrm{pix}}} \Psi(r_i)\Psi^*(r_j)$$

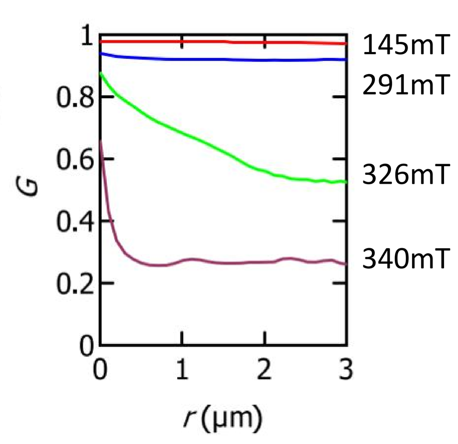

Conclusion

We have studied deformations in skyrmion lattices in a sample of FeGe by applying GPA to Lorentz TEM images. Deformation fields were measured around a single dislocation and were found to be in good agreement with deformation fields calculated using linear elasticity. Rotations were measured at the boundaries between skyrmion crystal grains and were also in accordance with a numerical model taking into account the distribution of the dislocations. Finally, an orientational order parameter and the corresponding correlation function were obtained from GPA maps. They were used to evaluate the disorder in a skyrmion lattice as a function of the applied magnetic field and study the different phases.

Methods

Experiments were carried out using a TFS Titan TEM equipped with a Schottky field emission gun operated at 300 kV, a CEOS image aberration corrector and a 4k*4k Gatan K2-IS direct electron detector. The microscope was operated in Lorentz mode by using the first transfer lens of the aberration corrector as the main imaging lens. The objective lens was used to apply magnetic fields perpendicular to the sample. A liquid-nitrogen-cooled specimen holder (Gatan model 636) was used to vary the sample temperature. The Digital Micrograph software and a GPA plugin were used to calculate deformation maps. A TEM lamella of FeGe was prepared from a bulk crystal using focused Ga^+ ion beam sputtering in a scanning electron microscope (FIB-SEM) TFS Helios dual-beam platform.